Cytoskeletal-based mechanisms differently regulate *in vivo* and *in vitro* proplatelet formation

Alicia Bornert,[1] Julie Boscher,[1] Fabien Pertuy,[1] Anita Eckly,[1] David Stegner,[2] Catherine Strassel,[1] Christian Gachet,[1] François Lanza[1] and Catherine Léon[1]

[1]Université de Strasbourg, INSERM, EFS Grand-Est, BPPS UMR-S 1255, Strasbourg, France and [2]Institute of Experimental Biomedicine, University Hospital Würzburg & Rudolf Virchow Center for Experimental Biomedicine, University of Würzburg, Würzburg, Germany

Ferrata Storti Foundation

ABSTRACT

Platelets are produced by bone marrow megakaryocytes through cytoplasmic protrusions, named native proplatelets (nPPT), into blood vessels. Proplatelets also refer to protrusions observed in megakaryocyte culture (cultured proplatelets [cPPT]) which are morphologically different. Contrary to cPPT, the mechanisms of nPPT formation are poorly understood. We show here in living mice that nPPT elongation is in equilibrium between protrusion and retraction forces mediated by myosin-IIA. We also found, using wild-type and β1-tubulin-deficient mice, that microtubule behavior differs between cPPT and nPPT, being absolutely required *in vitro*, while less critical *in vivo*. Remarkably, microtubule depolymerization in myosin-deficient mice did not affect nPPT elongation. We then calculated that blood Stokes' forces may be sufficient to promote nPPT extension, independently of myosin and microtubules. Together, we propose a new mechanism for nPPT extension that might explain contradictions between severely affected cPPT production and moderate platelet count defects in some patients and animal models.

Correspondence:

CATHERINE LÉON
catherine.leon@efs.sante.fr

Introduction

Blood platelets are key elements of hemostasis for the prevention of bleeding and are produced by a unique mechanism. They arise from megakaryocytes (MK), specialized cells in the bone marrow.[1,2] Upon differentiation from hematopoietic progenitors, MKs undergo endomitosis, leading to a giant cell, whose cytoplasm is filled by a highly developed intracellular membrane network called the demarcation membrane system (DMS).[3] At a mature stage, MK lie adjacent to the bone marrow sinusoid vessels and initiate cytoplasmic protrusion through the vessel wall. These protrusions further elongate inside the blood circulation, attached to their mother cells. These extensions are named proplatelets (PPT) and are fueled by the DMS that acts as a membrane reservoir to allow PPT growth.[4] Once inside the blood stream, PPT are released into the circulation as large fragments that have been proposed to further remodel in downstream organs to release bona fide platelets, small anucleated MK fragments having a discoid shape.[2,5,6]

The first PPT term was proposed following *in situ* scanning electron microscopy (SEM) observation of "long intrasinusoidal "proplatelet" processes which originate from the cell body of extravascularly located megakaryocytes".[7] Later on, *in vivo* observations by time lapse imaging in living animal confirmed the morphology of PPT as elongated protrusions in wild-type (WT) mice under physiological conditions.[7-14] The same denomination was also given to the cytoplasmic MK extensions in culture or in bone marrow explants.[8,15-19] Yet, the morphology of PPT observed *in vitro* strongly differs from that observed *in situ/in vivo*. Early *in vitro* observations of marrow explants[8,15,16,20] and later of progenitor-differentiated MK in culture[17,19,21] similarly recorded PPT presenting branched thin shafts (1-4 μm in diameter) leading to an entanglement of PPT surrounding the MK body.[17-19] These morphological differences between these two types of MK extensions raise the possibility that the mechanisms at stake could as well differ between *in vitro* cultured PPT (hereafter

referred as cPPT) and *in vivo* generated native PPTs (referred as nPPT).

While the mechanisms governing cPPT extension *in vitro* have been well documented, no study has clearly evaluated the *in vivo* cytoskeleton-based mechanisms regulating the extension of nPPT. Based on *in vitro* experiments, several cytoskeletal elements have been identified as playing a major role.[22,23] Inside cPPT, the microtubules are organized as linear bundles of mixed polarity running along the shaft and ending as a coil in the cPPT bud, prefiguring the platelet marginal band.[2,17,24] Incubating MK *in vitro* in the presence of microtubule depolymerizing drugs prevented de novo cPPT extension[17,21,25,26] and retracted already formed cPPT.[16,17,21] More recent work suggests that the sliding property of microtubules, rather than their proper polymerization, is the primary driver of cPPT extension.[11,24] On the other hand, actin has been proposed to play a role in the branching process since F-actin depolymerization reduces the number of bifurcations,[17] while myosin activity decreases the extension of cPPT and has no impact on their morphology except on the bud size.[26,27]

In the present study we examined whether the mechanisms previously described *in vitro* also apply to the nPPT by genetically and pharmacologically manipulating cytoskeletal key components. We show that in the bone marrow of living mice, the previously *in vitro* described mechanism governing nPPT extension differs from the previously one described *in vitro*.

Methods

For details see the *Online Supplementary Appendix.* This study was approved by the Local Ethical Committee and experiments were performed according to the Agreement for Experimentation released by the French government (Agreement numbers: 2016090911005304 and 2018061211274514).

Intravital imaging
Intravital imaging was performed with either *mT/mG;Pf4-cre* mice[28] or following MK and nPPT staining by intravenous injection of an AF488-conjugated anti-GPIX antibody derivative.[29] Two-photon microscopy was performed by observation of skull bone marrow as described.[29] Anesthetized mice where observed for a maximum of 3 hours (h), during which time one to four nPPT could be recorded.

In vitro proplatelet formation
Bone marrow experiments were performed as described.[26] *In vitro* liquid culture of Lin- mouse progenitors was performed as described previously.[30]

Immunofluorescence and confocal observations
Bone marrow experiments were performed as described.[26] *In vitro* liquid culture of Lin⁻ mouse progenitors was performed as described previously.[30]

Results

Distinct morphologies between *in vivo* native proplatelets and *in vitro* cultured proplatelets
As already shown by others,[4,7,9,10,31,32] nPPT extending into bone marrow sinusoids are unbranched and elongated protrusions that appear mostly larger than cPPT. nPPT extensions can be observed *in situ* in fixed tissues by GPIbβ immunolabeling or SEM (Figure 1Ai-iii, see also Figure 4C), clearly showing the slightly bulbous aspect of their ends (Figure 1A, ii and iii inset). As also previously shown by others, two-photon microscopy observations in living animal confirmed this elongated morphology, sometimes irregular with constriction zones, which extend over long distances (Figure 1Bi-iii; *Online Supplementary Video S1-3; Online Supplementary Figure S1A*). nPPT were rarely found to segment at their extremities, but rather broke off as long fragments subsequently further remodeled into individual platelets (*Online Supplementary Figure S1B*).

In contrast, the morphology of cPPT appears highly different. Using various microscopy techniques, cPPT observed *in vitro*, either from cultured MK or cultured marrow explants, present a regular thin shaft terminated by a bud (Figure 1Ci-iii). The cPPT shaft diameter is four-times smaller than the shafts measured on nPPT (Figure 1D), notwithstanding the different microscopy techniques used for their observations. The cPPT bud diameter is twice the size of the cPPT shaft (Figure 1D, left panel). Furthermore, the cPPT buds are already discoid as clearly visible by SEM (Figure 1Cii, arrows), prefiguring the future platelet, contrary to the nPPT ends (Figure 1Aii-iii).

These data that essentially confirm previous observations by others are presented for comparison purposes as these important PPT morphological differences between *in vitro* and *in vivo* observations suggest that the underlying mechanisms might be different. We therefore evaluated the role of the cytoskeleton in the dynamics of nPPT formation.

In vivo native proplatelet elongation dynamics are regulated by myosin IIA that opposes driving forces
As observed *in vivo* by two-photon microscopy, nPPT elongation is a dynamic and irregular process which proceeds through elongation periods interspersed with pause and retraction phases as exemplified in Figure 2A (red and blue traces) (see also the *Online Supplementary Figure S2B* for more tracings), resulting in high variability in elongation speed (*Online Supplementary Figure S2A*). We hypothesized that this irregular behavior resulted from opposing forces exerted by the cytoskeleton and that the myosin contractile cytoskeleton was a likely contributor. We previously showed that *Myh9⁻/⁻* mice had a quantitative defect in cPPT formation in the explant marrow model, with fewer MK extending PPT which were also less complex compared to WT mice.[26] Here using intravital microscopy, we were nevertheless able to find *Myh9⁻/⁻* extensions within sinusoids (Figure 2B). However, in contrast to WT nPPT, myosin-deficient cytoplasmic processes elongation occurred without any pause or retraction phases as exemplified in Figure 2C (*Online Supplementary Figure S2C*). Furthermore, the elongation speed was twice as high as that seen in WT nPPT, which might be explained by the absence of pauses and retractions (Figure 2D). Interestingly, *Myh9⁻/⁻* cPPT were longer and thinner (Figure 2 E-F). Their mean length was increased by 49% in *Myh9⁻/⁻* compared to WT nPPT and the shafts were 28% thinner. These findings suggest that myosin IIA, by increasing intracellular tension, renders the cytoplasmic extensions less stretchable and participates in the pauses and retractions observed under normal conditions.
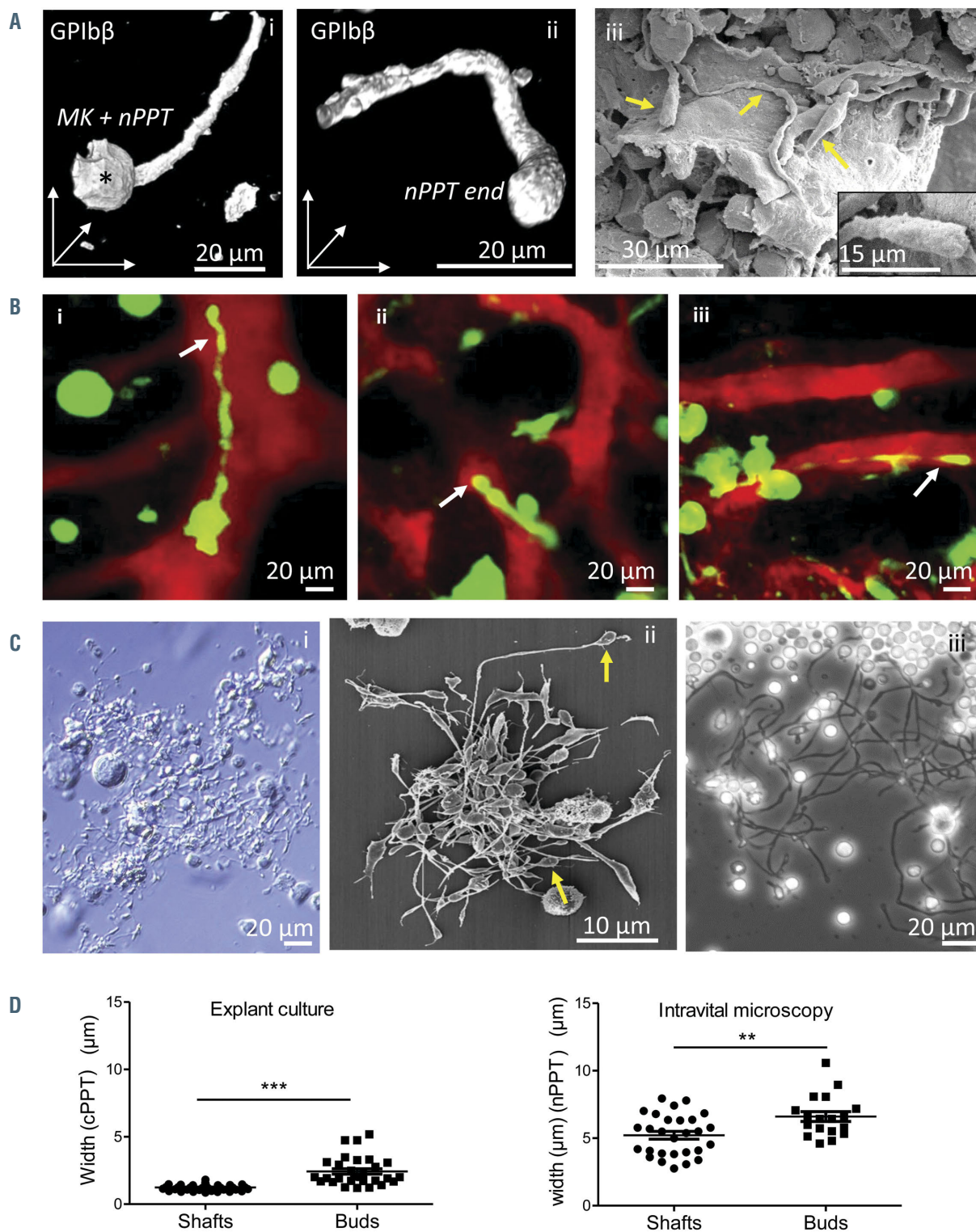
Figure 1. Native proplatelets generated in the bone marrow in vivo are morphologically different from cultured proplatelets. (A) Representative images of *in situ* bone marrow native proplatelets (nPPT): GPIbβ immunolabeling and confocal observation of a 30 μm-thick bone marrow section showing a portion of a long nPPT extending from the mother megakaryocyte (MK) (*) (i), and detail of a bulbous nPPT end (ii); images are 3D rendering using LASX software. (iii), several elongated nPPT (arrows) observed in a sinusoid vessel by scanning electron microscopy (SEM). Inset, magnification showing a bulbous nPPT end. Note the various nPPT shaft widths. Representative of at least three mice. (B) *In vivo* nPPT: z-projection images from time-lapse experiments showing the various morphologies of nPPT (arrows) extending within the bone marrow (BM) sinusoids. nPPT and MK are in green, sinusoid vessels are in red. Representative of at least 20 mice. (C) Representative images of *in vitro* cultured proplatelets (cPPT): cPPT produced by MK differentiated in culture from mouse BM progenitors, visualized by bright field microscopy at the bottom of the culture well before fixation (i) or after paraformaldehyde-fixation and SEM observation (ii); (iii), cultured proplatelets (cPPT) extending *in vitro* from a BM explant, observed by phase contrast microscopy. (D) Scatter plot representing cPPT shaft and terminal bud widths from explant BM measured on phase contrast images (left) (30-50 cPPT per group, data pooled from two individual BM explants) or nPPT shaft and terminal bud widths from *in vivo* recordings (right). Mean ± standard error of the mean from 18 to 28 values, pooled from 14 mice. Statistics analyzed using Mann-Whitney comparison test.

β1-tubulin deficiency prevents proplatelet formation *in vitro* but not *in vivo*

Among other key cytoskeletal elements, microtubules have been shown to play an essential role in the dynamics of cPPT. In order to determine their role *in vivo*, we used mice deficient in β1 tubulin (*Tubb1⁻/⁻*), the major β tubulin isoform in platelets. MK from *Tubb1⁻/⁻* mice were unable to extend protrusions *in vitro* in a bone marrow explant assay (Figure 3A, upper panel) and only rare abnormally short and compact extensions were observed following *in vitro* differentiation of bone marrow progenitors (Figure 3A, lower panel inset), confirming previous results in fetal liver-derived MK.[33]

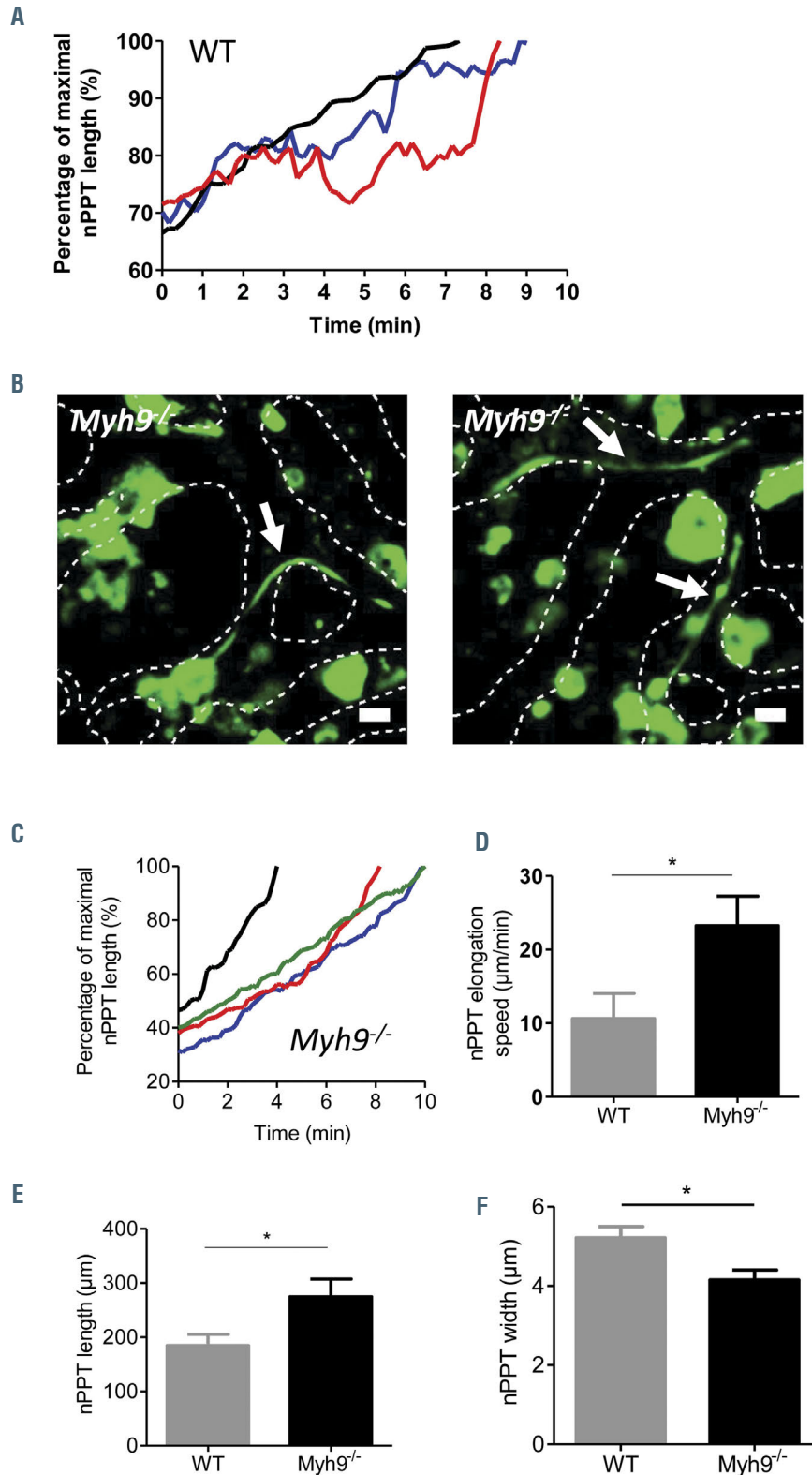*In situ*, examining the *Tubb1⁻/⁻* bone marrow by immuno-

Figure 2. Myosin regulates native proplatelet elongation speed. (A) Normalized native proplatelet (nPPT) length (%) of three independent wild-type (WT) mice plotted over time, showing regular elongation (black line, max length=282.1 μm), pauses between elongation phases (blue line, max length=151.2 μm) or pause and retraction phases between elongation phases (red line, max length =85.6 μm). Representative of nPPT from at least 10 WT mice. (B) Two z-projection images showing long, thin nPPT in *Myh9⁻/⁻* bone marrow sinusoids (arrows). Dotted lines represent the contours of the sinusoids. Scale bar =20 μm. Representative of at least 10 *Myh9⁻/⁻* mice. (C) Normalized length (%) of four representative *Myh9⁻/⁻* nPPT observed in three mice plotted over time, showing a continuous elongation, without pause or retraction (black line, max length =175.1 μm; green line, max length=221.2 μm; red line, max length=132.7 μm; blue line, max length=98.5 μm). (D) nPPT elongation speed. Data are 12 nPPT pooled from eight WT mice and 12 nPPT pooled from five *Myh9⁻/⁻* . (E) nPPT length. Data are 25 nPPT from 14 WT mice) and 13 nPPT from five *Myh9⁻/⁻* mice. (F) nPPT width close to the base of PPT. Data are 28 nPPT from 19 WT mice and 17 nPPT from eight *Myh9⁻/⁻*- mice. (D-F) Bar graphs represent the mean ± standard error of the mean; *P*-values were calculated using Mann-Whitney test.
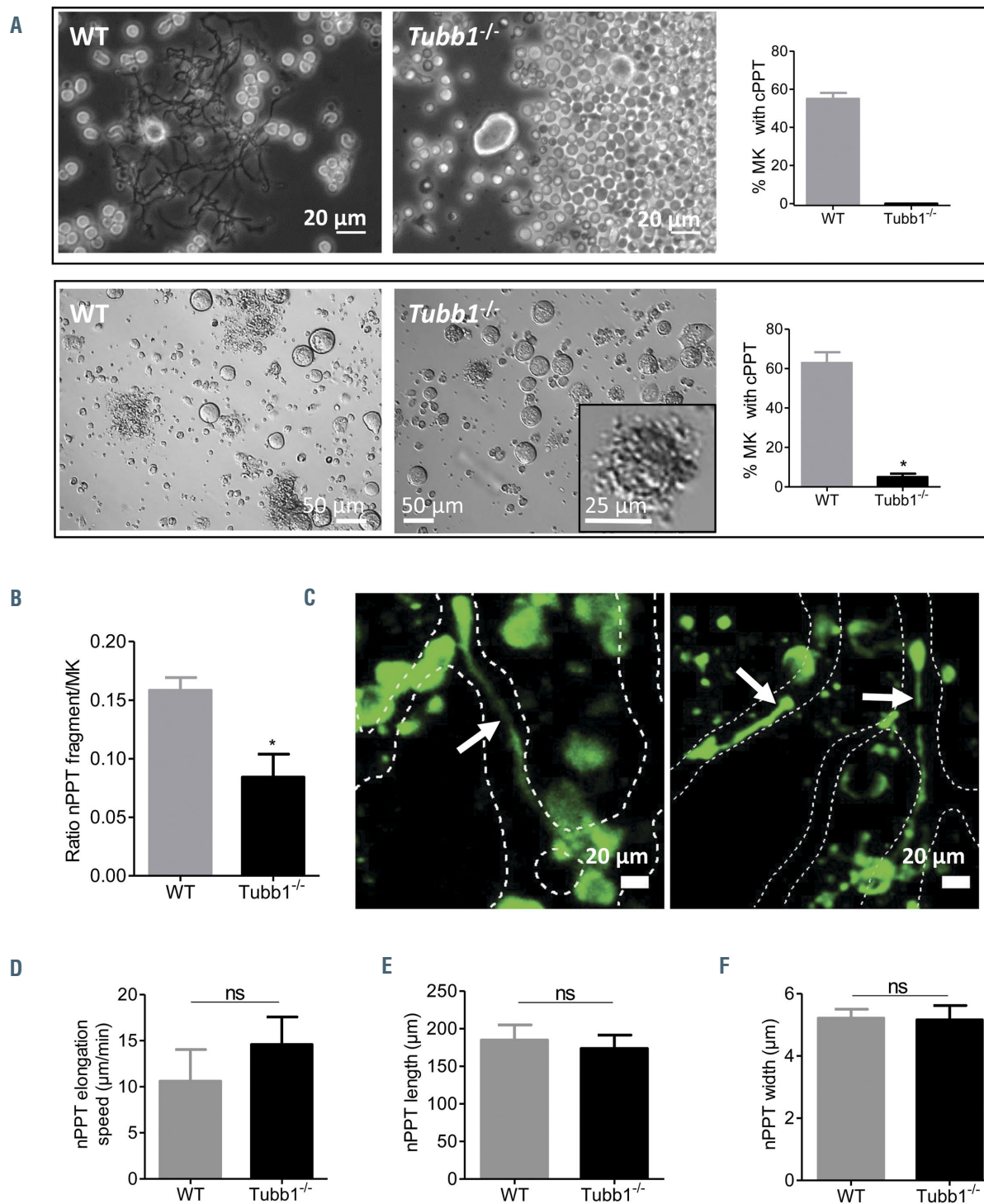
Figure 3. Strong discrepancy between *in vitro* cultured proplatelet formation and *in vivo* native proplatelet formation in *Tubb1⁻ᐟ⁻* mice. (A) Upper panel, explant bone marrow culture experiment. Representative phase contrast images and quantification of the percent of megakaryocytes (MK) presenting with cultured proplatelets (cPPT) after 6 hours of culture showing total absence of *Tubb1⁻ᐟ⁻* MK with protrusions (0%) while 55% of wild-type (WT) MK extended cPPT (mean ± standard error of the mean [SEM], n=3 independent experiments). Lower panel, MK forming PPT after 4 days of Lin⁻ progenitor culture. Representative bright field images and quantification of the percent of MK presenting with cPPT (mean ± SEM, n=4 independent experiments). Inset, rare *Tubb1⁻ᐟ⁻* MK forming abnormal cPPT without shaft extensions. (B) Estimation of the nPPT formation capacity in situ by calculating the ratio of PPT fragments over the total number of MK observed in 30-μm thick marrow sections. Bars are mean ± SEM of three to four independent marrow sections from two mice, representing 374 and 687 MK for WT and *Tubb1⁻ᐟ⁻*, respectively. (C) Two z-projection images of *in vivo Tubb1⁻ᐟ⁻* native proplatelets (nPPT). Dotted lines delimit the sinusoids. Representative of at least 12 nPPT from five mice. (D) nPPT elongation speed. Data are mean ± SEM of 16 nPPT pooled from eight WT mice and 12 nPPT pooled from four *Tubb1⁻ᐟ⁻* mice. (E) nPPT length. Data are mean ± SEM of 25 nPPT pooled from 14 WT mice and 16 nPPT pooled from five *Tubb1⁻ᐟ⁻* mice. (F) nPPT width. Data are mean ± SEM of 28 nPPT pooled from 19 WT mice and 16 nPPTs pooled from five *Tubb1⁻ᐟ⁻* mice. Bar graphs represent the mean ± SEM; all data analyzed using Mann-Whitney test. ns: not significant.
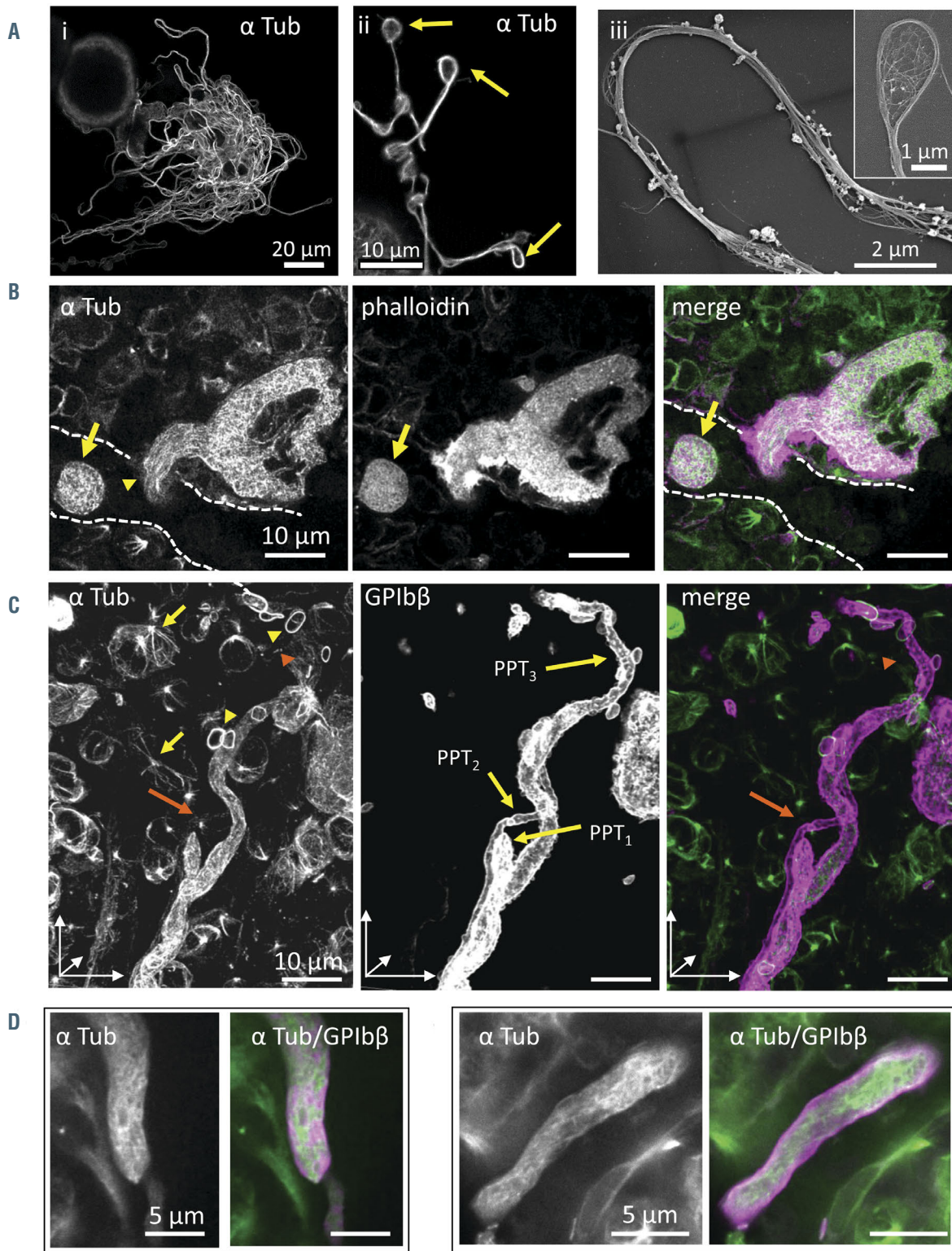
Figure 4. Microtubules are differentially distributed along proplatelets *in situ* compared to *in vitro*. (A) i-ii: cultured proplatelets (cPPT) from wild-type (WT) megakaryocytes (MK) differentiated in culture for 4 days, labeled with an antibody against α tubulin. iii: microtubule bundles within the cPPT shaft and coils in the bud (inset), observed by scanning electron microscopy (SEM) after the removal of the membrane by treatment with Triton X-100. (B) Confocal images of a nascent native proplatelets (nPPT) within bone marrow 30-μm thick sections revealing an absence of microtubule bundle organization (antibodies against α tubulin in green) and F-actin (phalloidin labeling, in magenta). Dotted lines represent sinusoid vessel. Note the presence of an nPPT transversally sectioned (arrow) in the sinusoid, again lacking microtubule bundles. (C-E) *In situ* bone marrow nPPT immunolabeling with antibodies against α tubulin (green) and GPIbβ (magenta). (C) 3D visualization of z-stack (30 μm thick) showing parts of three entangled nPPT after GPIbβ labeling, denoted PPT_1, PPT_2 and PPT_3. Tubulin labeling was discontinuous being weak to absent in certain portions of the nPPT. For example, labeling becomes weaker in the upper part of the longest nPPT (PPT_3) (orange arrowhead). Tubulin labeling in the thinnest nPPT (PPT_2) was hardly visible in our settings (orange arrow). Marginal band of platelets (yellow arrowheads) and mitotic spindles (yellow arrows) were well labeled denoting well-preserved microtubules. (D-E) Confocal single-plane images at higher magnification showing nPPT portions. Note that the microtubules are not arranged longitudinally. (B-E) Representative of four wild-type (WT) femur bone marrow from two mice.

labeling, we found that the number of MK was increased by around 75% compared to the WT mice (*Online Supplementary Figure S3A*), probably as a compensatory response to the thrombocytopenia (*Online Supplementary Figure S3B*). *Tubb1⁻ᐟ⁻* mouse MK were able to extend protrusions in marrow sinusoids, although we found a 45% decrease in the number of nPPT extensions compared to WT nPPT, in agreement with the decreased number of circulating platelets (Figure 3B; *Online Supplementary Figure S3B*). *Tubb1⁻ᐟ⁻* nPPT exhibited a fully normal morphology (Figure 3C) with a surprisingly normal elongation speed (Figure 3D) and a fully normal mean length and width (Figure 3E-F). These results indicate that while the absence of an essential tubulin isoform almost totally abrogates PPT formation *in vitro*, it partially affects the number of

PPT *in vivo* but not their elongation speed. Overall, this points to different mechanisms contributing to PPT extension when considering the *in vivo* situation with a less crucial importance of microtubules compared to *in vitro*.

Microtubules are non-uniformly distributed in proplatelets *in vivo*

Another difference between *in vivo* and *in vitro* was observed by looking at the cytoplasmic distribution of microtubules. Within cPPT obtained *in vitro*, microtubules are organized into a bundle running along the shaft as previously described[17] and as illustrated in Figure 4A. We then explored their organization *in situ* under conditions that preserved microtubules as denoted by the intact marginal band of platelets and mitotic spindles in marrow cells (see
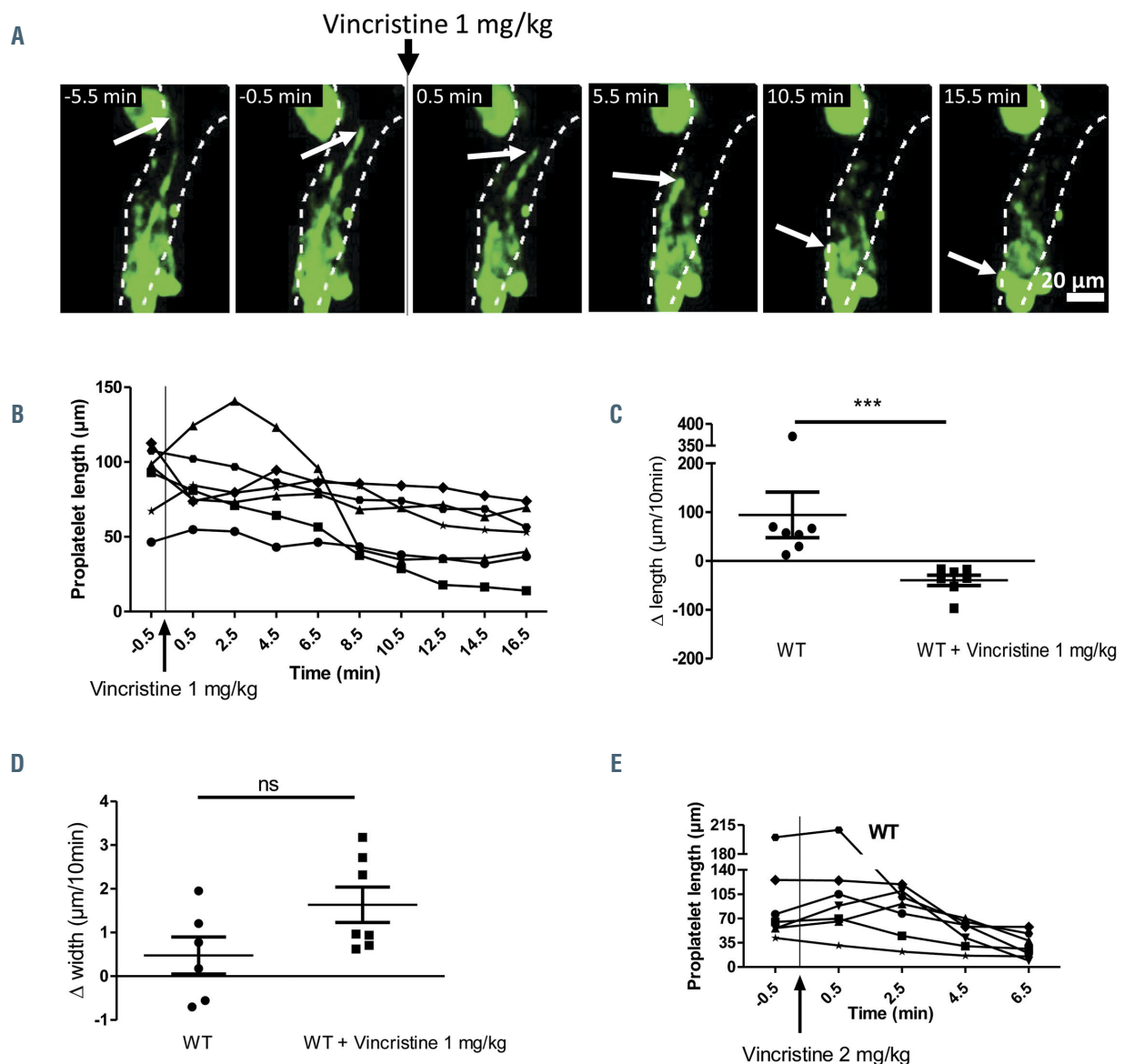

Figure 5. **Vincristine infusion leads to shrinkage of preformed wild-type native proplatelets.** A) Representative z-projection time-lapse images showing an native proplatelets (nPPT) before and after vincristine administration (1 mg/kg). (B) Length of individual nPPT plotted as a function of time before and after 1 mg/kg vincristine administration. Seven mice analyzed. (C) Scatter plot of nPPT length difference during a 10-minute observation showing elongation in the absence of vincristine and retraction following vincristine injection (from 0.5-10.5 min). Seven mice were analyzed for each condition. (D) Measurement of the difference in width close to the base during a 10-minute window showing small positive or negative variation in the absence of vincristine (left) and increasing width following vincristine injection (right). Seven mice were analyzed. (E) Doubling the vincristine dose administration accelerates nPPT shrinkage. Seven mice were analyzed. All data analyzed using Mann-Whitney test. ns: not significant.

on Figure 4C yellow arrowheads and arrows). As shown in Figure 4B (left, arrowhead), microtubules were not organized as bundles but aligned roughly parallel in the direction of the extension in nascent nPPT. This different microtubule organization suggests a different role in the process of nPPT extension. Of note, strong F-actin labeling was observed laterally at the site of transmigration, indicating also the importance of this cytoskeleton in this first step (Figure 4B, middle). Focusing on later stages in the elongated nPPT, we observed that again, unlike *in vitro*, the microtubules were not arranged in large bundles running along the extension, and microtubules were not longitudinally aligned in parallel but were found in various non-uniform orientations along the nPPT (Figure 4B arrow; Figure 4C-E; especially compare Figure 4Aii with Figure 4B-C which

have the same scale). As seen in Figure 4C showing a three-dimensional (3D) view of three portions of intertwined nPPT, the labelling was not always constant, being sometimes decreased (Figure 4C left, orange arrowhead) or even absent (Figure 4C left, orange arrow), suggesting few microtubules and mainly non-polymerized tubulin. Hence the difference between the *in vivo* and *in vitro* role of microtubules in the process of MK extension is further illustrated by the difference in microtubule organization/distribution within nascent and elongating nPPT compared to cPPT.

Administration of vincristine leads to shrinkage of preexisting wild-type proplatelets

In a second approach, and because *Tubb1*$^{-/-}$ mice compensate the β1 tubulin deficiency by overexpressing β2
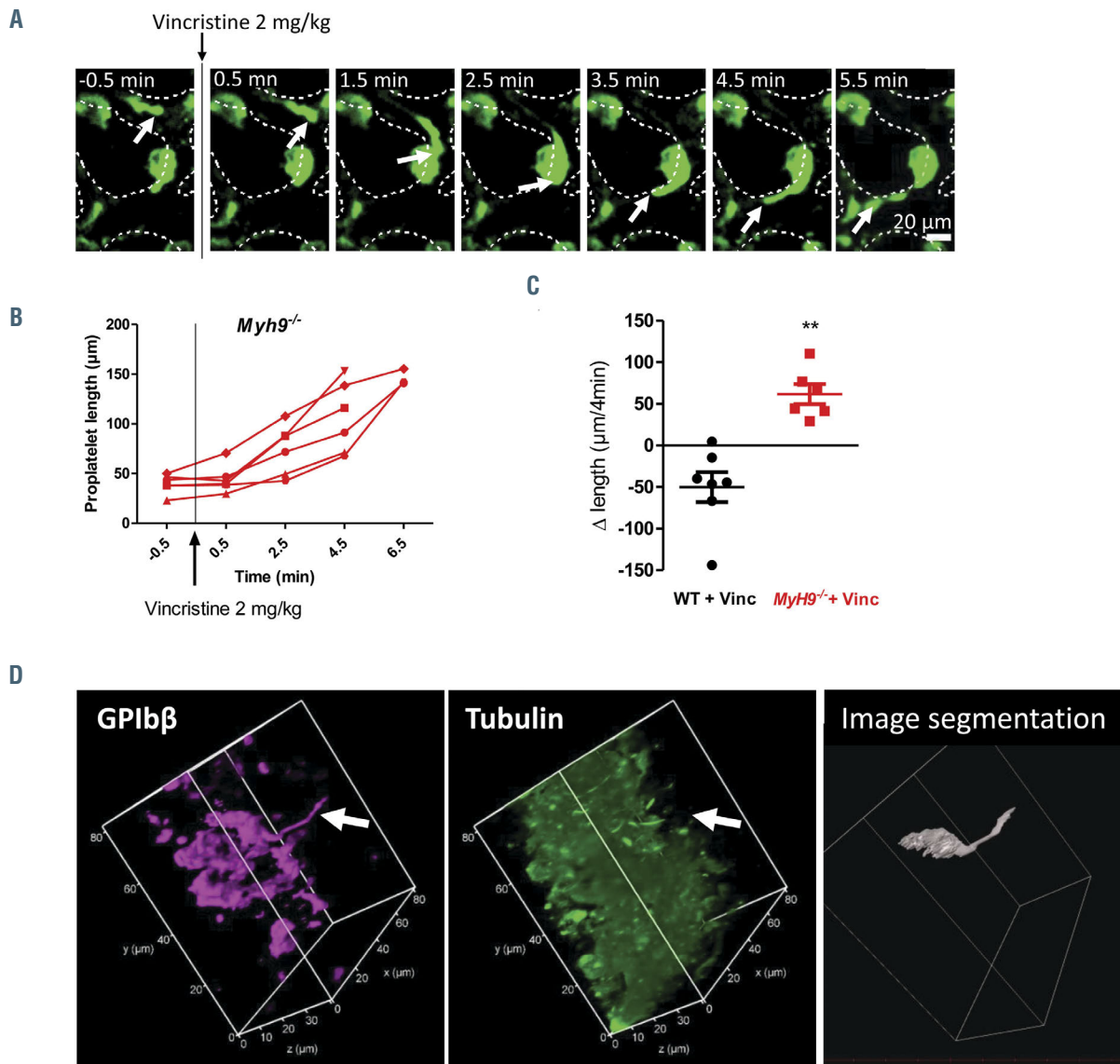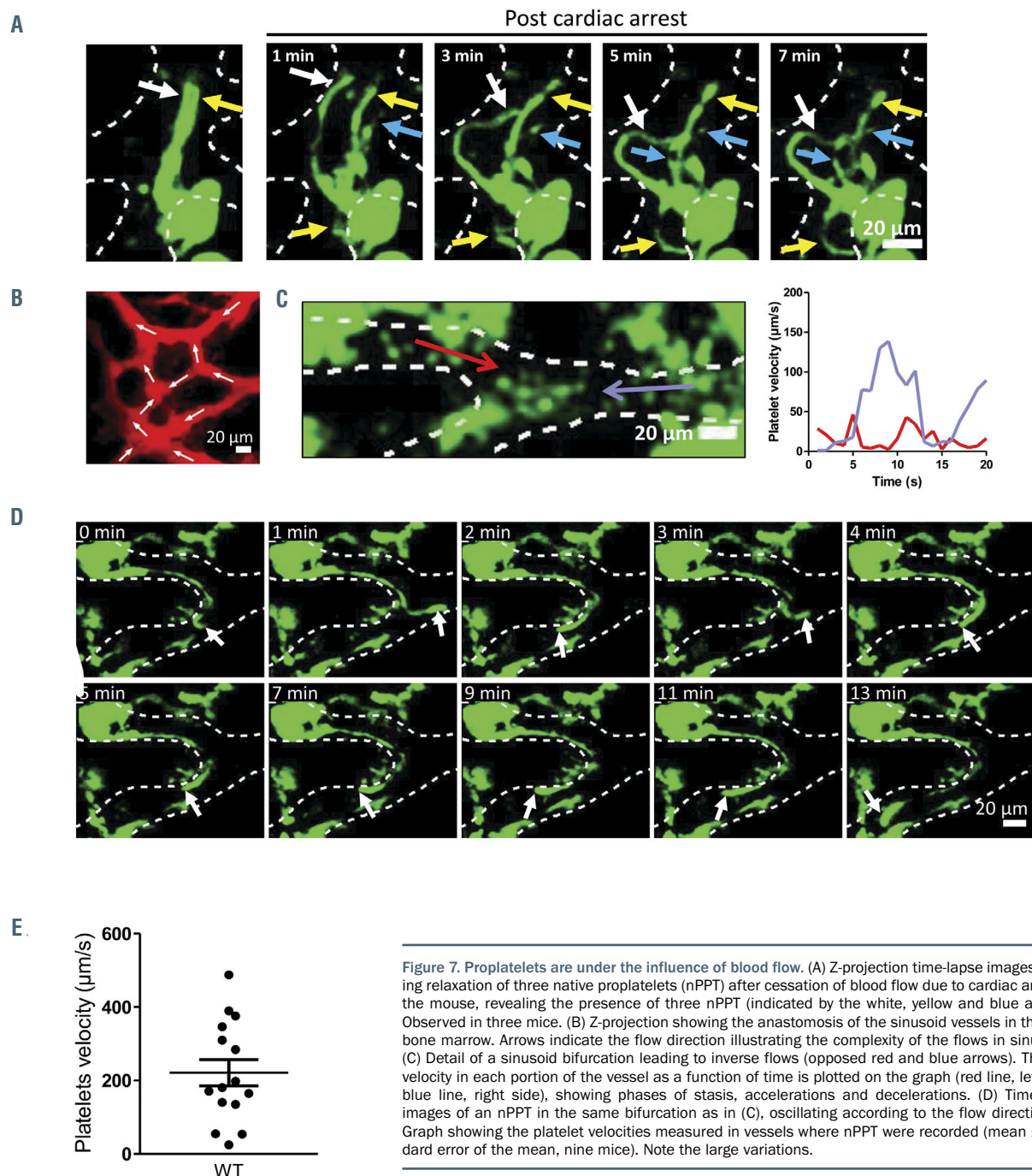

Figure 6. *Myh9*$^{-/-}$ native proplatelets still elongate after vincristine administration. (A) Representative z-projection time-lapse images showing *Myh9*$^{-/-}$ protrusions before and after vincristine administration. (B) Measurement of protrusions length in *Myh9*$^{-/-}$ mice before and after 2 mg/kg vincristine administration plotted as a function of time. Note that some Myh9-/- protrusions could not be recorded after 4.5 minutes since they escaped the observation field. Six mice were analyzed. (C) Measurement of the difference in length during a 4-minute window (0.5–4.5 minutes post 2 mg/kg vincristine injection), showing retraction in wild-type (WT) mice and elongation in *Myh9*$^{-/-}$ mice. Seven WT mice and six *Myh9*$^{-/-}$ mice analyzed, using Mann-Whitney statistical analysis. (D) Immunolabeling of bone marrow sections from *Myh9*$^{-/-}$ mice injected with vincristine (1 mg/kg) 10 minutes prior to the removal of the femurs and fixation of the bone marrow, showing the absence of microtubule labeling in a long protrusion (arrow). Left, Magenta labeling showing GPIbβ; center, green labeling showing α tubulin; images represent a 3D view. Right panel, 3D representation of the megakaryocytes (MK) extending the nPPT obtained by image segmentation and 3D reconstruction with AMIRA software.

and β5 tubulin isotypes,[33] we pharmacologically depolymerized microtubules within preformed nPPT. Microtubule depolymerization was induced during the course of nPPT elongation by injecting the microtubule-destabilizing drug vincristine into WT mice (1 mg/kg). At this dose, vincristine induces depolymerization of microtubules from the marginal band of circulating platelets and from marrow cells in the extravascular compartment (Online *Supplementary Figure S4; Online Supplementary Figure S5*). Time-lapse recordings showed that the majority of preformed nPPT underwent shrinkage within 10 minutes after vincristine administration as illustrated in Figure 5A and *Online Supplementary Video S4*, and quantified in Figure 5B-D. Most nPPT progressively became

shorter (Figure 5A-C) and increased their thickness, especially at their base (Figure 5D). In some cases, the shrank fragments were captured on time-lapse recordings while they were released into circulation. Doubling the vincristine dose (2 mg/kg) accelerated PPT shrinkage to as early as 2 minutes after drug administration (Figure 5E). These results indicate that the microtubule cytoskeleton is required to maintain the nPPT elongated morphology once it is formed.

Microtubules are dispensable for *Myh9*^{-/-} proplatelet elongation

Given that myosin IIA is required for the retraction phases observed in WT nPPT, we investigated whether

Figure 7. Proplatelets are under the influence of blood flow. (A) Z-projection time-lapse images showing relaxation of three native proplatelets (nPPT) after cessation of blood flow due to cardiac arrest of the mouse, revealing the presence of three nPPT (indicated by the white, yellow and blue arrows). Observed in three mice. (B) Z-projection showing the anastomosis of the sinusoid vessels in the skull bone marrow. Arrows indicate the flow direction illustrating the complexity of the flows in sinusoids. (C) Detail of a sinusoid bifurcation leading to inverse flows (opposed red and blue arrows). The flow velocity in each portion of the vessel as a function of time is plotted on the graph (red line, left side; blue line, right side), showing phases of stasis, accelerations and decelerations. (D) Time-lapse images of an nPPT in the same bifurcation as in (C), oscillating according to the flow direction. (E) Graph showing the platelet velocities measured in vessels where nPPT were recorded (mean ± standard error of the mean, nine mice). Note the large variations.

the shrinkage observed after injection of vincristine was dependent on myosin contractility. Again, we previously controlled that microtubules from *Myh9^-/-^* mouse platelets and MK were sensitive to vincristine-induced depolymerization (*Online Supplementary Figure S4; Online Supplementary Figure S5*). Strikingly, no PPT shrinkage occurred after vincristine administration in *Myh9^-/-^* mice, rather the protrusions continued to elongate so rapidly that they often disappeared from the observation field within 10 minutes (*Online Supplementary Video S5; Online Supplementary Figure S6*). Increasing vincristine dose to 2 mg/kg did not modify this surprising behavior, as again none of the *Myh9^-/-^* protrusions retracted, and elongation continued (Figure 6A-C).

Examination of the bone marrow sections by immunofluorescence microscopy showed that *Myh9^-/-^* nPPT, like their WT counterparts, do not present a unique microtubule bundle (*Online Supplementary Figure S7,* to compare to Figure 4D-E). Treatment with vincristine did not prevent the observation of long GPIbβ-positive protrusions despite the lack of visible microtubules (Figure 6D, arrow). These data indicate that the shrinkage following microtubule depolymerization is dependent on active myosin IIA.

Altogether these data show that in the absence of myosin IIA, microtubules were totally dispensable for nPPT elongation, indicating that elongation can be promoted by other driving forces, independent of microtubules.

Stokes' forces can contribute to native proplatelets elongation

Driving forces contributing to the elongation process could originate from blood flow. This hypothesis was initially supported by the observation that cessation of blood flow induced the relaxation of already preformed three nPTT that extended in the same flow line (Figure 7A; *Online Supplementary Video S6*), showing that blood flow maintains nPPT under tension.

Flows in sinusoids are complex due to the intricate anastomosis of the vasculature (Figure 7B). This was evidenced during the monitoring of platelet movements inside vessels of living mice as in some cases areas of inverse flows were observed (Figure 7C; *Online Supplementary Video S7*). In these areas, nPPT were tossed from one branch of a vessel to another, without PTT detachment (Figure 7D; *Online Supplementary Video S8*). Since they remain attached to the stationary MK in the bone marrow, nPPT are submitted to the fluid force of the flowing blood all along their shafts and buds. Assuming the nPPT end as a sphere, the force can be calculated using the Stokes' formula $F = 6\pi\eta LV$ where L is the radius of the sphere, V the velocity of the fluid and η the viscosity. The Stokes' force applied to the nPPT end was estimated based on the displacement of circulating platelets, recorded in vessels where nPPT were extended (V=213 μm/s (range: 24-488) (Figure 7E). The nPPT end having a mean radius of 4 μm
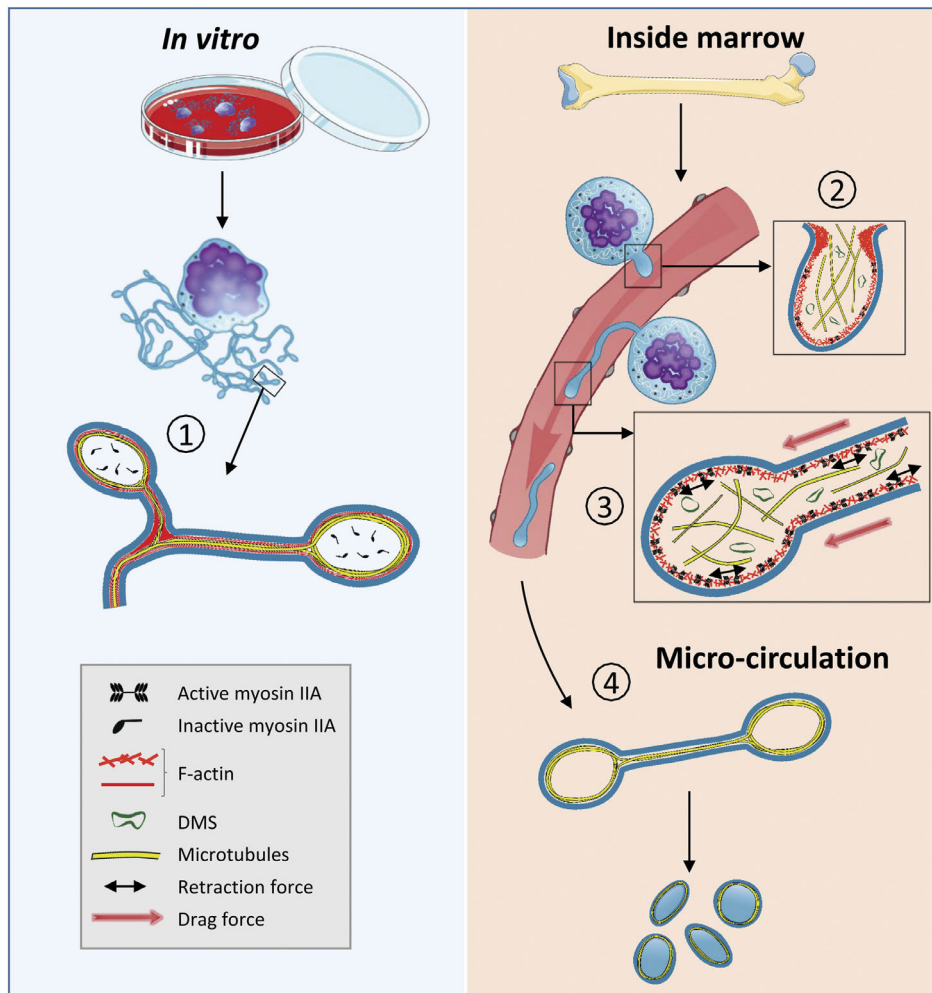

Figure 8. The proposed model depicting the cytoskeletal-based differences between *in vivo* and *in vitro* proplatelet formation. In cultured proplatelets (cPPT) generated *in vitro*, initiation and elongation depend essentially on the microtubule cytoskeleton organized as linear bundles along the PPT shafts and ending as a coil (1), already prefiguring the marginal band of the future platelets, while F-actin would promote branching. *In vivo*, the initiation of native proplatelets (nPPT) formation takes place in the marrow and depends on both actin and microtubule cytoskeletons (2). During nPPT elongation in the sinusoid circulation, microtubules do not form a unique bundle but are mostly isolated and play a critical role to counteract myosin-based nPPT retraction (3), while drag forces contribute to the protrusive forces. The released elongated nPPT fragments are further remodeled in the downstream microcirculation resulting in the final circulating platelets, possibly through microtubule-based mechanisms similar to in vitro mechanisms (4). DMS: demarcation membrane system.

(L) and the apparent viscosity η of the blood in microvessels varying from $2-4\times10^{-3}$ Pa.s,[34-36] the Stokes' force is approximatly 30-60 pN on the bud. This value can be considered as the minimal force as the Stokes' force is also applied all along the nPPT shaft. It is known from the literature that a force around 20-50 pN is usually required to extend membrane nanotubes in cells including blood cells such as neutrophils or erythrocytes.[37-39] Hence the force exerted by the blood flow on the whole nPPT would be high enough to substantially contribute to nPPT extension.

Discussion

In this study we evaluated the mechanisms of nPPT formation as it occurs *in vivo* inside bone marrow sinusoid vessels. We found that the mechanisms differ from those taking place in order to produce cPPTs under *in vitro* conditions, especially with regards to the relative implication of two main cytoskeletal components, i.e., microtubules and myosin. We show that the non-continuous nPPT elongation process resulting from pause and retraction phases resulted from myosin IIA. MK are known to activate myosin IIA in response to local increase in shear.[40,41] Blood flow within sinusoid vessels presents heterogeneous shear stresses ranging from zero to 10 dyn/cm², [42,43] generating forces that are sufficient to trigger cellular mechanotransduction in endothelial cells.[44] Hence, depending on the flow forces, transient myosin activation could increase membrane tension to preserve its integrity. Conversely, a decreased myosin IIA activity would increase membrane compliance and stretching, promoting thinner and longer protrusions such as observed in *Myh9*⁻ᐟ⁻ mice. Another hypothesis could be that myosin-promoted pauses serve to slow down the extension process in order for DMS to properly enter the nPPT. In favor of this hypothesis, we observed *in situ* that myosin-deficient nPPT contain very few DMS membranes compared to WT ones (*Online Supplementary Figure S8*), which could also explain the thinner morphology of these *Myh9*⁻ᐟ⁻ nPPT.

Unexpectedly, the microtubule behavior was found to differ between nPPT and cPPT. This was first revealed in *Tubb1*⁻ᐟ⁻ mice *in vivo*. Although the number of MK extending nPPT was decreased, in agreement with the moderate thrombocytopenia, their morphology and elongation speed were fully normal. This was in stark contrast to the almost total inability of *Tubb1*⁻ᐟ⁻ MK to form cPPT *in vitro*. These findings are a further indication that the defects of *Tubb1*⁻ᐟ⁻ mice are exacerbated *in vitro* and they are clear evidence of mechanistic differences between the two environments.

Given these observations, we hypothesize that MK extensions generated *in vivo* are less dependent on microtubules than anticipated from cPPT produced *in vitro*. We observed that microtubules were present in the nascent nPPT, although not organized in bundles, as also previously mentioned in an earlier work.[8] Their presence however suggested that they might still play a role in nPPT initiation, in agreement with the decreased number of *Tubb1*⁻ᐟ⁻ nPPT observed *in situ. In vivo*, the precise intracellular mechanisms controlling the initiation and transmural passage of nPPTs are still unknown. The first step of nPPT extension, which initiates in the marrow stroma and in the absence of blood forces, might require higher protrusive forces to push against the endothelial barrier compared to liquid culture. It is most probable that both F-actin and microtubule cytoskeletons jointly play a role as we also observed strong F-actin accumulation in MK at the site where the nascent nPPT cross the vessel wall (Figure 4B). This F-actin accumulated in structures resembling shoulder-like structures which could correspond to the fibrillary-rich collars previously observed by Behnke and Forer and could be an anchorage point for facilitating the initial protrusion.[31,4] At this stage, whether microtubules directly contribute together with F-actin to promote the initial pushing force for the transmural passage, or whether they are indirectly required to organize vesicle/organelle transport to bring essential components or play a role as information carriers for F-actin is not known.[45]

Upon subsequent nPPT growth inside sinusoids, we observed a non-uniform distribution of microtubules inside elongated nPPT which clearly differs from the microtubule bundles uniformly lining the cPPT shafts and ending as coils observed *in vitro*. Although we were beyond the resolution limit to see microtubule arrangement in areas of strongest nPPT constriction *in situ*, these were clearly observed as unbundled in larger areas, in agreement with early observations by Behnke mentioning random arrangement in large clumps of MK cytoplasm released in sinusoids *in situ*.[8] Radley and Scurfield also observed *in situ* that microtubules were aligned in constriction zones but splayed out on either side of the constriction.[46] These results confirm and extend those recently published by Brown *et al*. showing by tomography that *in situ*, microtubules were individual and randomly distributed in MK protrusions.[4] Hence all the above data point to a different mechanism depending on whether MK extend protrusions *in vitro* or *in vivo*. However, microtubules are clearly important for maintaining the elongated nPPT structure in WT mice. This was evidenced here after inducing *in vivo* microtubule depolymerization on preexisting nPPT.

A much unexpected observation in *Myh9*⁻ᐟ⁻ mice was the continuous growth of MK protrusions within sinusoids even when microtubules were depolymerized by vincristine. This indicated that under conditions where contractile forces are weakened, abrogating nPPT retraction, elongation of protrusions is still occurring. Hence, inside the blood vessels, microtubules would be less crucial for nPPT elongation. Isolated microtubules have a low pushing force in the range of 3-4 pN, while it has been demonstrated that organization in bundles increases their force-generating capacity in an additive fashion.[47-49] While *in vitro* microtubule bundles could conceivably be the primary driving force for elongation, this is different *in vivo* where the essential role of microtubules would be to act as a backbone to transport constituents and to prevent and counteract myosin-mediated nPPT retraction. Of note, *Tubb1*⁻ᐟ⁻ platelets do not present abnormalities in their granule distribution (see the *Online Supplementary Figure S3C*) contrary to knockout mice having actomyosin impairments,[32,50] showing that partial microtubule content is sufficient to promote normal organelle transport into the maturing MK and the nPPT.

Our finding then raised the question of the force promoting MK fragment elongation *in vivo*. Our data suggest that the main motor for nPPT elongation may come from hemodynamic forces. The importance of blood flow was

previously noted by data showing increased cPPT elongation velocity under flow compared to static conditions,[11,51] and from our observations that nPPT always align in the direction of flow, especially visible upon inverse flows (*Online Supplementary Video S8*) or when flow stopped (*Online Supplementary Video S6*; Figure 7). Even with low blood flow velocities as in sinusoids, ranging from about ten to several hundred µm/s[42,43] (Figure 7E), we calculated that the Stokes' force exerted on the nPPT end would be sufficient to stretch the membrane.[37-39] The same force, applied all along the PPT shaft, would further increase the overall driving force and promote its extension. Taking into account the fact that DMS fuses with the plasma membrane all along the nPPT shaft as shown by Brown *et al.*,[4] this continuous membrane replenishment most probably considerably decreases membrane tension as demonstrated in other systems,[52,53] thus even further lowering the forces required for nPPT elongation.

Our findings do not exclude a key role of microtubules in the final platelet formation. We may speculate that this final nPPT remodeling into barbell platelets and final platelets could occur through microtubule-based mechanisms, similar to those previously established in liquid culture,[6,11] leading to microtubule coils prefiguring the marginal band. In favor of this idea, Lefrançais *et al.* recently published some videos of free MK fragment remodeling in lung vessels that produced extensions strikingly resembling branched cPPT extended by MK in culture.[5] In addition, we could observe that *in situ* barbell platelets and free nPPT fragments share a microtubule organization similar to cPPT including microtubules coils (personal observation and [54]).

It is apparent from the present work added to earlier data, that the cytoplasmic processes of MK are structurally different *in vivo* and *in vitro* due to the different mechanisms leading to their extension. The question then arises as to the respective nomenclature of these extensions. Should the term PPT be used for extensions within the bone marrow or for the extensions observed in *in vitro* systems, or even for MK fragments released into the circulation and which are truly "pro"-platelets? Defining distinct nomenclatures for each of these structures might help to get a clearer picture of thrombopoiesis in pathophysiology compared to the *in vitro* platelet production process. We propose that large MK fragments extended *in vivo* are named "nPPT" for native PPT, as opposed to "cPPT" for cultured PPT present *in vitro*.

We therefore propose a model for the nPPT formation in the bone marrow that differs from the one established *in vitro*. *In vivo*, while microtubules may contribute to the initial cytoplasmic extension of the nascent nPPT, they appear to be far less important for the elongation process once the nPPT is inside the blood flow. Microtubules rather play a role as a backbone to prevent nPPT retraction mediated by actomyosin contraction. nPPT elongation per se could proceed through blood drag forces that stretch nPPT plasma membrane as it is fueled by the DMS. We propose that this *in vivo* mechanism which occurs in the native and complex marrow environment, is bypassed in the liquid culture conditions. The *in vitro* microtubule-based mechanisms previously described potentially takes place at a later second time point, once nPPT have been released inside the blood circulation (Figure 8). Taken together, these data may explain why in some cases, strong discrepancies were observed between the capacity to extend cPPT, quantified *in vitro*, compared to the moderately decreased circulating platelet count.[33,55,56] Our work may thus help to understand the mechanisms of thrombocytopenia in patients especially when mutations occur in cytoskeletal proteins.

References

1. Kaushansky K. Thrombopoiesis. Semin Hematol. 2015;52(1):4-11.
2. Machlus KR, Thon JN, Italiano JE Jr. Interpreting the developmental dance of the megakaryocyte: a review of the cellular and molecular processes mediating platelet formation. Br J Haematol. 2014;165(2):227-236.
3. Eckly A, Heijnen H, Pertuy F, et al. Biogenesis of the demarcation membrane system (DMS) in megakaryocytes. Blood. 2014;123(6):921-930.
4. Brown E, Carlin LM, Lo Celso C, Poole AW. Multiple membrane extrusion sites drive megakaryocytes migration into bone marrow blood vessels. Life Sci Alliance. 2018; 1(2):1-12.
5. Lefrancais E, Ortiz-Munoz G, Caudrillier A, et al. The lung is a site of platelet biogenesis and a reservoir for haematopoietic progenitors. Nature. 2017;544(7648):105-109.
6. Thon JN, Italiano JE Jr. Does size matter in platelet production? Blood. 2012; 120(8):1552-1561.
7. Becker RP, De Bruyn PP. The transmural passage of blood cells into myeloid sinusoids and the entry of platelets into the sinusoidal circulation; a scanning electron microscopic investigation. Am J Anat. 1976;145(2):183-205.
8. Behnke O. An electron microscope study of the rat megacaryocyte. II. Some aspects of platelet release and microtubules. J Ultratruct Res. 1969;26(1):111-129.
9. Junt T, Schulze H, Chen Z, et al. Dynamic visualization of thrombopoiesis within bone marrow. Science. 2007; 317(5845): 1767-1770.
10. Kowata S, Isogai S, Murai K, et al. Platelet demand modulates the type of intravascular protrusion of megakaryocytes in bone marrow. Thromb Haemost. 2014; 112(4): 743-756.
11. Bender M, Thon JN, Ehrlicher AJ, et al. Microtubule sliding drives proplatelet elongation and is dependent on cytoplasmic dynein. Blood. 2015;125(5):860-868.
12. Nishimura S, Nagasaki M, Kunishima S, et al. IL-1alpha induces thrombopoiesis

through megakaryocyte rupture in response to acute platelet needs. J Cell Biol. 2015;209(3):453-466.

13. Zhang L, Orban M, Lorenz M, et al. A novel role of sphingosine 1-phosphate receptor S1pr1 in mouse thrombopoiesis. J Exp Med. 2012;209(12):2165-2181.

14. Zhang L, Urtz N, Gaertner F, et al. Sphingosine kinase 2 (Sphk2) regulates platelet biogenesis by providing intracellular sphingosine 1-phosphate (S1P). Blood. 2013;122(5):791-802.

15. Leven RM, Yee MK. Megakaryocyte morphogenesis stimulated in vitro by whole and partially fractionated thrombocytopenic plasma: a model system for the study of platelet formation. Blood. 1987;69(4):1046-1052.

16. Radley JM, Haller CJ. The demarcation membrane system of the megakaryocyte: a misnomer? Blood. 1982;60(1):213-219.

17. Italiano JE, Jr., Lecine P, Shivdasani RA, Hartwig JH. Blood platelets are assembled principally at the ends of proplatelet processes produced by differentiated megakaryocytes. J Cell Biol. 1999;147(6):1299-1312.

18. Eckly A, Strassel C, Cazenave JP, Lanza F, Leon C, Gachet C. Characterization of megakaryocyte development in the native bone marrow environment. Methods Mol Biol. 2012;788:175-192.

19. Pouli D, Tozzi L, Alonzo CA, et al. Label free monitoring of megakaryocytic development and proplatelet formation in vitro. Biomed Opt Express. 2017;8(10):4742-4755.

20. Thiery JP, Bessis M. Genesis of blood platelets from the megakaryocytes in living cells. C R Hebd Seances Acad Sci. 1956;242(2):290-292.

21. Tablin F, Castro M, Leven RM. Blood platelet formation in vitro. The role of the cytoskeleton in megakaryocyte fragmentation. J Cell Sci. 1990;97(Pt 1):59-70.

22. Ghalloussi D, Dhenge A, Bergmeier W. New insights into cytoskeletal remodeling during platelet production. J Throm Haemost. 2019;17(9).

23. Poulter NS, Thomas SG. Cytoskeletal regulation of platelet formation: coordination of F-actin and microtubules. Tint J Biochem Cell Biol. 2015;66:69-74.

24. Patel SR, Richardson JL, Schulze H, et al. Differential roles of microtubule assembly and sliding in proplatelet formation by megakaryocytes. Blood. 2005;106(13):4076-4085.

25. Handagama PJ, Feldman BF, Jain NC, Farver TB, Kono CS. In vitro platelet release by rat megakaryocytes: effect of metabolic inhibitors and cytoskeletal disrupting agents. Am J Vet Res. 1987;48(7):1142-1146.

26. Eckly A, Rinckel JY, Laeuffer P, et al. Proplatelet formation deficit and megakaryocyte death contribute to thrombocytopenia in Myh9 knockout mice. J Thromb Haemost. 2010;8(10):2243-2251.

27. Eckly A, Strassel C, Freund M, et al. Abnormal megakaryocyte morphology and proplatelet formation in mice with megakaryocyte-restricted MYH9 inactivation. Blood. 2009;113(14):3182-3189.

28. Pertuy F, Aguilar A, Strassel C, et al. Broader expression of the mouse platelet factor 4-cre transgene beyond the megakaryocyte lineage. J Thromb Haemost. 2015;13(1):115-125.

29. Stegner D, vanEeuwijk JMM, Angay O, et al. Thrombopoiesis is spatially regulated by the bone marrow vasculature. Nat Commun. 2017;8(1):127.

30. Strassel C, Eckly A, Leon C, et al. Hirudin and heparin enable efficient megakaryocyte differentiation of mouse bone marrow progenitors. Exp Cell Res. 2012;318(1):25-32.

31. Behnke O, Forer A. From megakaryocytes to platelets: platelet morphogenesis takes place in the bloodstream. Eur J Haematol Suppl 1998;61:S3-23.

32. Pertuy F, Eckly A, Weber J, et al. Myosin IIA is critical for organelle distribution and F-actin organization in megakaryocytes and platelets. Blood. 2014;123(8):1261-1269.

33. Schwer HD, Lecine P, Tiwari S, Italiano JE Jr., Hartwig JH, Shivdasani RA. A lineage-restricted and divergent beta-tubulin isoform is essential for the biogenesis, structure and function of blood platelets. Curr Biol. 2001;11(8):579-586.

34. Popel AS, Johnson PC. Microcirculation and hemorheology. Ann Rev Fluid Mech. 2005;37:43-69.

35. Pries AR, Secomb TW. Microvascular blood viscosity in vivo and the endothelial surface layer. Am J Physiol Heart Circ Physiol. 2005; 289(6):H2657-2664.

36. Lipowsky HH. Microvascular rheology and hemodynamics. Microcirculation. 2005;12(1):5-15.

37. Borghi N, Brochard-Wyart F. Tether extrusion from red blood cells: integral proteins unbinding from cytoskeleton. Biophys J. 2007;93(4):1369-1379.

38. Hochmuth RM, Marcus WD. Membrane tethers formed from blood cells with available area and determination of their adhesion energy. Biophys J. 2002;82(6):2964-2969.

39. Shao JY, Hochmuth RM. Micropipette suction for measuring piconewton forces of adhesion and tether formation from neutrophil membranes. Biophys J. 1996;71(5):2892-2901.

40. Shin JW, Swift J, Spinler KR, Discher DE. Myosin-II inhibition and soft 2D matrix maximize multinucleation and cellular projections typical of platelet-producing megakaryocytes. Proc Natl Acad Sci U S A. 2011;108(28):11458-11463.

41. Spinler KR, Shin JW, Lambert MP, Discher DE. Myosin-II repression favors pre/pro-platelets but shear activation generates platelets and fails in macrothrombocytopenia. Blood. 2015;125(3):525-533.

42. Bixel MG, Kusumbe AP, Ramasamy SK, et al. Flow dynamics and HSPC homing in bone marrow microvessels. Cell Rep. 2017;18(7):1804-1816.

43. Mazo IB, von Andrian UH. Adhesion and homing of blood-borne cells in bone marrow microvessels. J Leukoc Biol. 1999;66(1):25-32.

44. Chao Y, Ye P, Zhu L, et al. Low shear stress induces endothelial reactive oxygen species via the AT1R/eNOS/NO pathway. J Cell Physiol. 2018;233(2):1384-1395.

45. Dent EW, Baas PW. Microtubules in neurons as information carriers. J Neurochem. 2014;129(2):235-239.

46. Radley JM, Scurfield G. The mechanism of platelet release. Blood. 1980;56(6):996-999.

47. Dogterom M, Yurke B. Measurement of the force-velocity relation for growing microtubules. Science. 1997;278(5339):856-860.

48. Kolomeisky AB, Fisher ME. Force-velocity relation for growing microtubules. Biophys J. 2001;80(1):149-154.

49. Vleugel M, Kok M, Dogterom M. Understanding force-generating microtubule systems through in vitro reconstitution. Cell Adh Migr. 2016;10(5):475-494. through in vitro reconstitution. Cell Adh Migr. 2016;10(5):475-494.

50. Bender M, Eckly A, Hartwig JH, et al. ADF/n-cofilin-dependent actin turnover determines platelet formation and sizing. Blood. 2010;116(10):1767-1775.

51. Dunois-Larde C, Capron C, Fichelson S, Bauer T, Cramer-Borde E, Baruch D. Exposure of human megakaryocytes to high shear rates accelerates platelet production. Blood. 2009;114(9):1875-1883.

52. Gauthier NC, Masters TA, Sheetz MP. Mechanical feedback between membrane tension and dynamics. Trends Cell Biol. 2012;22(10):527-535.

53. Wang G, Galli T. Reciprocal link between cell biomechanics and exocytosis. Traffic. 2018;19(10):741-749.

54. Thon JN, Italiano JE. Platelet formation. Semin Hematol. 2010;47(3):220-226.

55. Strassel C, Eckly A, Leon C, et al. Intrinsic impaired proplatelet formation and microtubule coil assembly of megakaryocytes in a mouse model of Bernard-Soulier syndrome. Haematologica. 2009;94(6):800-810.

56. Strassel C, Magiera MM, Dupuis A, et al. An essential role for alpha4A-tubulin in platelet biogenesis. Life Sci Alliance. 2019;2(1):e201900309.